

网络出版时间: 2023-09-19 16:12:43 网络出版地址: <https://link.cnki.net/urlid/34.1065.R.20230918.1415.031>

◇口腔医学研究◇

骀贴面的预备设计和纤维桩对穿髓型楔状缺损抗折性分析

张雨晴^{1,2} 陈如婷^{1,2} 武郭敏^{1,2} 张红艳^{1,2}

摘要 目的 探讨不同骀贴面的预备设计和纤维桩对穿髓型楔状缺损的上颌前磨牙断裂载荷和断裂模式的影响。方法 将60颗上颌第一前磨牙随机分为纤维桩组和树脂组,每组30颗。纤维桩组用玻璃纤维桩和树脂核修复,树脂组仅用树脂核填充。分别用骀贴面(G2)、颊骀贴面(G3)和颊邻骀贴面(G4)修复离体牙,将复合树脂充填(G1)和全冠修复(G5)的牙齿分别设为阴性和阳性对照,每组6颗。牙齿经过5 000次冷热循环和20 000次垂直压缩载荷老化。再对所有牙齿以0.5 mm/min的速度进行静态加载,直至断

裂。记录下来每颗牙齿的断裂载荷和断裂模式。结果 纤维桩组和树脂组的组内断裂载荷均为 $G5 > G3 > G2 > G4 > G1$,且 $G2$ 、 $G3$ 、 $G4$ 、 $G5$ 的断裂载荷显著高于 $G1$,差异有统计学意义($P < 0.05$)。与树脂组比较,纤维桩组组间断裂载荷差异无统计学意义($P > 0.05$)。 $G3$ 断裂形式多为修复体脱粘接,有利于再次修复。结论 颊骀贴面修复穿髓型楔状缺损牙齿的效果最理想,纤维桩不能显著增强穿髓型楔状缺损牙齿的断裂载荷。

关键词 骀贴面; 楔状缺损; 断裂载荷; 断裂模式

中图分类号 R 783.3

文献标志码 A 文章编号 1000-1492(2023)10-1786-07

doi: 10.19405/j.cnki.issn1000-1492.2023.10.031

2023-05-19 接收

基金项目: 安徽省高校自然科学基金项目(编号: KJ2020A0165); 安徽医科大学口腔医学院资助—峰原提升项目(编号: 2022xkfyts10)

作者单位: ¹ 安徽医科大学口腔医学院, 安徽医科大学附属口腔医院, 安徽省口腔疾病研究重点实验室, 合肥 230032

² 安徽医科大学附属口腔医院牙体牙髓科, 合肥 230032

作者简介: 张雨晴, 女, 硕士研究生;

张红艳, 女, 副教授, 硕士生导师, 责任作者, E-mail: toothyan@126.com

楔状缺损是指牙齿唇、颊颈部硬组织缓慢消耗所致的缺损。严重的楔状缺损可导致牙髓炎和根尖周炎, 根管治疗(root canal therapy, RCT)将会进一步降低牙齿的抗折力^[1], 从而使应力集中在缺损处, 极易发生牙齿横折。目前治疗穿髓型楔状缺损的方法有复合树脂填充、桩冠法等, 但都有一定的局

with the risk of type 2 diabetic nephropathy (DN). **Methods** The clinical data of 215 patients with type 2 diabetes mellitus (T2DM) were collected and analyzed. According to the results of estimated glomerular filtration rate (eGFR) and urinary albumin to creatinine ratio (UACR), they were divided into 117 patients with T2DM and 98 patients with DN. The clinical data, biochemical indicators and continuous glucose monitoring (CGM) indicators of the two groups were compared. Logistic regression was used to analyze the influencing factors of DN risk. The predictive value of TIR and GMI on the risk of DN was evaluated by receiver operating characteristic (ROC) curve. **Results** There were significant differences in age, duration of diabetes, systolic blood pressure, glycosylated hemoglobin (HbA1c), fasting plasma glucose (FPG), 2 hour postprandial plasma glucose (2hPG), creatinine (Cr), UACR, eGFR between the two groups ($P < 0.05$). There were statistically significant differences between the two groups in the CGM indexes of GMI, mean absolute difference of mean of daily differences (MODD), glucose above target range time (TAR) and TIR ($P < 0.05$). The results of logistic regression analysis showed that TIR was a protective factor of DN. In the ROC curve analysis of TIR prediction DN, the area under the ROC curve was 0.718 (95% CI = 0.648 ~ 0.789, $P < 0.001$), and the Yoden index was 0.38. At this time, the sensitivity was 66.7%, and the specificity was 71.3%. In the ROC curve analysis of GMI prediction DN, the area under the ROC curve was 0.701 (95% CI = 0.629 ~ 0.774, $P < 0.001$), and the Yoden index was 0.368. At this time, the sensitivity was 63.3%, and the specificity was 73.5%. **Conclusion** TIR and GMI are significantly associated with the risk of DN. Specifically, lower TIR and higher GMI increase the risk of DN.

Key words type 2 diabetic nephropathy; time in range; glucose management indicator; continuous glucose monitoring

限性^[2]。复合树脂的聚合收缩易导致充填体断裂和继发龋。研究^[3]表明,桩冠法存活率明显高于树脂充填法,但全冠预备去除了大量的牙体组织,从而降低牙齿抗折力^[4]。随着粘接技术的快速发展,微创修复已成为一种较好延长牙齿寿命的治疗选择。殆贴面是一种主要依靠粘接固位的微创修复体。临床研究表明^[5],用殆贴面修复严重磨损的后牙存活率可达90%以上。为了更好地恢复磨损牙齿的外观和功能,设计了咬合面、舌面和近远中面覆盖的多种功能性殆贴面。然而,目前尚无关于不同预备形式的殆贴面在RCT后穿髓型楔状缺损牙齿治疗上的研究。因此,该研究制备了3种不同预备形式的殆贴面,并以树脂充填为阴性对照,以全冠为阳性对照,探究殆贴面和纤维桩对RCT后穿髓型楔状缺损的牙齿断裂载荷及模式的影响,为临床上治疗提供相关参考。

1 材料与方法

1.1 主要材料与仪器 0.5% 氯胺-T 溶液购自西格玛奥德里奇(上海)贸易有限公司; 0.5% 次氯酸钠溶液、生理盐水购自朗力生物医药(武汉)有限公司; 15% 磷酸酸蚀剂购自德国 Gluma Etch 公司; 5% 氢氟酸酸蚀剂购自美国皓齿制品有限公司; 乙二胺四乙酸(ethylene diamine tetraacetic acid, EDTA) 凝胶购自韩国 Vericom 公司; Filtek Z350XT 流体树脂、RelyX Fibre Post 纤维桩、纤维桩钻、Express STD 硅橡胶、RelyX Ulal Clicker 冠粘接剂购自美国 3M ESPE 公司; 双固化树脂购自美国 MEDENTAL 公司; 自凝树脂购自上海二医张江生物材料有限公司; 10 号 K 锉购自瑞士 Dentsply Maillefer 公司; 25 mm 欧罗德卡镍钛锉购自意大利 Orodeka 公司; 热牙胶充填系统购自深圳慈恩齿科口腔管理有限公司; P 钻购自深圳市德嘉医疗器械有限公司; IPS e. max CAD 购自瑞士 Ivolar Vivadent 公司; 聚四氟乙烯生料带、PVC 塑料管购自北京渡美科技发展有限公司; 电热

水浴箱购自上海博讯实业有限公司; 锥形压头、RGM-6010 型万能试验机购自深圳瑞格尔仪器有限公司; LEICAEZ4HD 光学显微镜购自德国 LEICA 公司。

1.2 牙齿收集 在安徽医科大学伦理委员会的批准下(伦理批号: HM2022004), 收集年轻成人用于正畸目的的上颌第一前磨牙。牙齿在显微镜下仔细观察, 选择 60 颗进行实验。纳入标准: 尺寸相似; 根尖孔闭合, 单根和双根管; 无龋病、牙齿无裂纹、缺损和根管吸收。仔细刮去牙石、菌斑后, 在 4℃ 下于 0.5% 氯胺-T 溶液中保存 1 周。

1.3 牙齿分组与制备 对 60 颗牙齿进行严重的缺损制备和 RCT。缺损的总高度定为 3 mm, 上边缘顶点定为釉牙骨质界(cemento-enamel junction, CEJ)冠方 2 mm 处, 下边缘顶点定为 CEJ 根方 1 mm 处, 尖端位于 CEJ 根方 1 mm 处, 颊颈部深度为颊舌颈距离的 1/3, 最深处穿通髓腔。去除缺损区并打磨锐边, 冲洗干燥后使用 3M 流体树脂充填。用 10 号手用 K 锉畅通根管后测长, 根管工作长度设为距解剖性根尖孔 0.5 mm。使用 25 mm 的欧罗德卡镍钛机扩锉配合 EDTA 凝胶将根管预备为连续的锥形, 预备间隔用 0.5% 次氯酸钠溶液冲洗。根管预备完成后试尖, 干燥, 使用热牙胶充填系统封填牙胶至根管口。所有的牙齿根充完毕后, 随机均分为纤维桩组和树脂组($n=30$)。纤维桩组依次用 1、2 号 P 钻去除颊侧根管上部的牙胶, 在根尖处保留 4.0 mm 的充填物, 用黄色纤维桩钻将颊侧根管上部预备成型, 预备间隔用生理盐水冲洗降温。干燥后在管壁及髓室内涂布粘接剂后光固化 30 s, 将双固化树脂均匀涂布在髓室及桩体表面, 排出气泡后从咬合方向光固化 60 s, 于咬合面处切断纤维桩。树脂组直接充填双固化树脂, 上述步骤由同一名研究员完成, 以最大限度的减小误差。最后拍摄根尖片, 以确保充填效果符合要求。缺损预备充填图及根尖片, 见图 1。



图1 缺损预备、充填图及 RCT 和纤维桩后根尖片

A、B: 缺损预备图; C: 缺损充填图; D: RCT 后根尖片; E: RCT 和纤维桩后根尖片

将纤维桩组和树脂组各分为 5 小组 (G1、G2、G3、G4、G5), 每组 6 个牙齿。预备前用 3M 硅橡胶做出每颗牙齿的牙冠阴模, 便于精准控制预备量。对照组 G1 不做处理, G2、G3、G4、G5 分别用瓷贴面、颊瓷贴面、颊邻瓷贴面和全冠预备。瓷贴面 (G2): 将咬合面均匀降低 1.2 ~ 1.5 mm (牙尖 1.5 mm, 中央窝 1.2 mm); 颊瓷贴面 (G3): 咬合面的预备方法与 G2 相同, 颊面的厚度减至 0.5 ~ 1.2 mm, 去除倒凹, 并在缺损底部边缘下方 0.5 mm 处预备 0.5 mm 的浅凹型肩台; 颊邻瓷贴面 (G4): 咬合面、颊面和肩台的预备与 G3 相同, 近远中面的厚度减至 1.0 ~ 1.5 mm, 确保轴面无倒凹, 聚合角为 6°; 全冠 (G5): 咬合面均匀降低 1.5 ~ 2.0 mm (牙尖处为 2.0 mm, 中央窝处为 1.5 mm), 颊舌面和近远中面均匀降低 1.0 ~ 1.5 mm。颊侧缘位于楔状缺损底边缘根向 1.0 mm 处, 舌侧缘位于 CEJ 处, 形成 1.0 mm 的浅凹型肩台, 去除所有倒凹, 聚合角为 6°, 修复体预备后和预备量示意图见图 2。

1.4 修复体制作与粘接 用 CAD/CAM 系统对预备好的牙齿进行扫描, 忽略咬合面复杂的窝沟间隙。精确测量修复体的厚度, 进行基牙试戴, 确保完全就位且边缘密合。按照 3M 冠粘接剂的使用说明, 在修复体内表面涂抹 5% 氢氟酸蚀剂 30 s, 冲洗 30 s, 吹干。G2、G3、G4 组基牙表面涂抹 15% 磷酸酸蚀

剂 30 s, 冲洗干燥。同 G5 组一起于基牙表面涂布粘接剂 20 s, 吹干 5 s 后, 光固化 20 s, 将绿巨人粘接剂均匀涂抹于基牙和修复体内表面。准确对位后, 用手指按压并光固化。

1.5 牙齿老化与静载 所有牙齿在 5 ~ 55 °C 之间进行 5 000 次冷热循环, 每个温度 30 s, 期间暂停 3 s。然后用 0.2 mm 的聚四氟乙烯生料带覆盖在 CEJ 以下 2 mm 的牙根部以模拟牙周膜。将自凝树脂在室温下混合, 于面团期填充于 PVC 塑料管, 将牙根埋至 CEJ 下 2 mm 处模拟牙槽骨, 放置 24 h, 使其完全凝固。定制锥形压头为锥角 50°, 顶部 4 mm 的半球压头。室温下, 于万能试验机上以 1 mm/min 的速度对牙齿中央窝施加 20 000 个压缩载荷, 大小为 100 N, 频率为 2 Hz。循环结束时, 在光学显微镜下仔细检查所有样品是否有裂缝。在相同的万能试验机上, 以 0.5 mm/min 的速度对牙齿施加垂直静态载荷。当压缩曲线出现第 1 个骤降转折点时, 计算机系统自动停止加压, 记录断裂载荷并保存断裂曲线。每组的断裂载荷以 N 为单位记录。静载后, 拍摄牙齿断裂的光学图, 并用光学显微镜对裂纹进行评价。断裂模式^[6]为: I 型: 修复体中广泛的裂纹形成; II 型: 修复体的粘接断裂; III 型: 修复体和 CEJ 以上牙齿的断裂; IV 型: 修复体和 CEJ 以下牙齿的纵向断裂。见图 3。

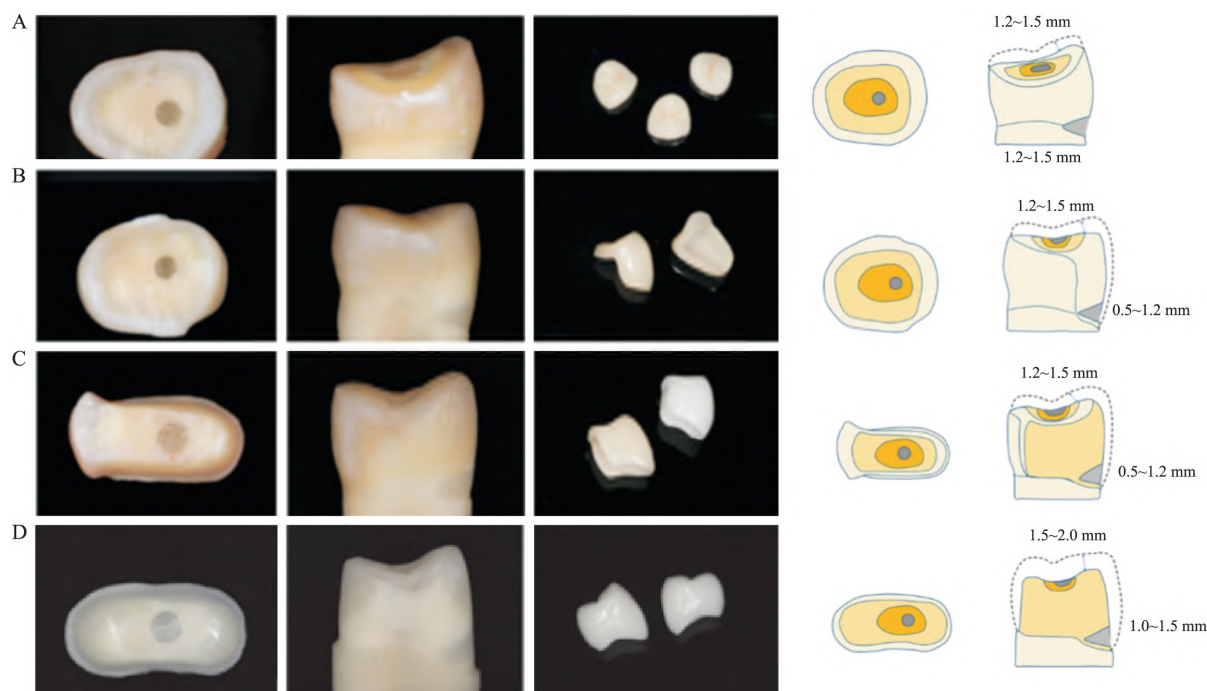


图 2 牙齿预备图及预备量

A: 瓷贴面; B: 颊瓷贴面; C: 颊邻瓷贴面; D: 全冠

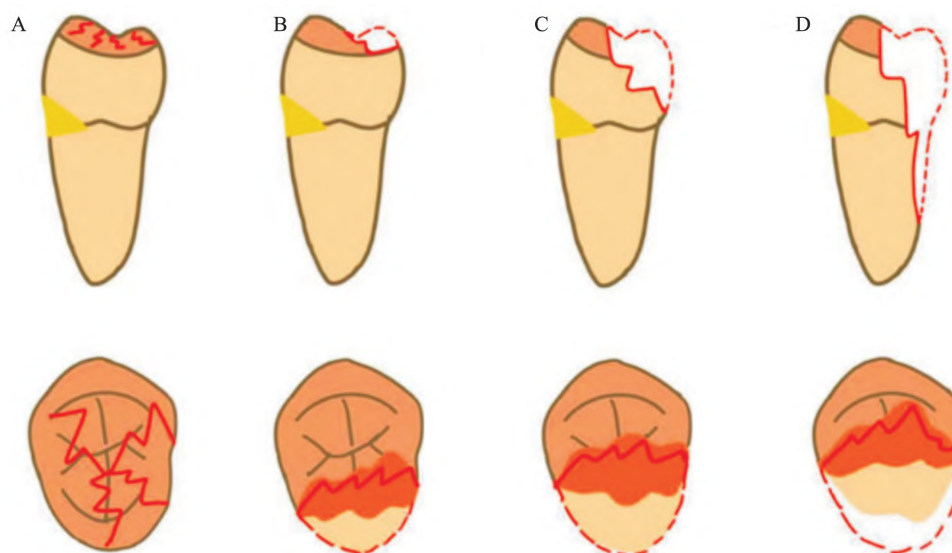


图3 以瓷贴面为例的断裂模式示意图

A: I型; B: II型; C: III型; D: IV型

1.6 统计学处理 用 GraphPadPrism8. 2. 1 对数据进行处理, 计算并记录各组断裂载荷的平均值。对数据进行正态检验后, 分别对不同牙齿预备形式、纤维桩组和树脂组的组内及组间断裂载荷进行单因素方差分析, $\alpha = 0.05$ 。对各组牙齿的断裂模式进行统计分析。

2 结果

所有牙齿在5 000冷热循环和20 000次循环压缩载荷下老化后均未出现裂纹。各组牙齿断裂载荷平均值见表1。

纤维桩组和树脂组的断裂载荷由大到小排列均为: G5 > G3 > G2 > G4 > G1, 经修复体修复后(G2、G3、G4、G5)的断裂载荷都高于未修复组(G1)。树脂组: G1和G2、G3、G4、G5比较, 差异有统计学意义($P < 0.05$); G2、G3、G4和G5比较, 差异有统计学意义($P < 0.05$); 纤维桩组: G1和G2、G3、G4、G5比较, 差异有统计学意义($P < 0.05$); G4和G5比较, 差异有统计学意义($P < 0.05$)。见表2、3。纤维

桩组和树脂组组间两两比较的显著性结果显示, 仅G4组组间断裂载荷比较差异有统计学意义($P < 0.05$)。

牙齿断裂模式的统计图见图4。如图4所示, 83%的牙齿的断裂模式是III型和IV型, 即牙齿和修复体的断裂。其中, G5有83%的牙齿为IV型断裂, 不能再次修复, 且牙冠横折占比较高。G2不可修复的比例为75%, 仅次于G5。而G3、G4牙齿大部分为有利修复, 不可修复的比例较低, 断裂形式多为修

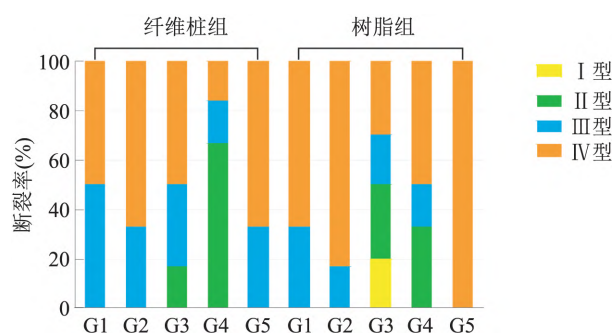


图4 断裂模式统计图

表1 各组断裂载荷平均值及最大值(N)

组别	树脂组			纤维桩组		
	$\bar{x} \pm s$	最小值	最大值	$\bar{x} \pm s$	最小值	最大值
G1	1 221.981 ± 147.829	1 012.465	1 223.422	1 453.962 ± 411.596	994.288	1 952.902
G2	2 196.737 ± 238.686	1 924.921	2 464.292	2 606.225 ± 203.048	2 312.291	2 755.454
G3	2 228.540 ± 156.435	2 029.545	2 405.763	2 628.134 ± 308.259	2 244.865	2 985.572
G4	1 660.238 ± 217.726	1 383.618	1 895.265	2 072.413 ± 147.159	1 927.725	2 272.375
G5	2 750.045 ± 171.108	2 538.099	2 917.311	2 707.824 ± 267.599	2 384.071	2 991.895

表 2 树脂组组内显著性的 LSD 分析检验

因变量	控制组	对比组	平均差	标准误	P 值	95% CI	
						下限值	上限值
树脂组	G1	G2	-974.755 75	134.156 03	0	-1 260.702 6	-688.808 9
		G3	-1 006.559 00	134.156 03	0	-1 292.505 8	-720.612 2
		G4	-438.256 50	134.156 03	0.005	-724.203 3	-152.309 7
		G5	-1 528.064 25	134.156 03	0	-1 814.011 1	-1 242.117 4
	G2	G1	974.755 75	134.156 03	0	688.808 9	1 260.702 6
		G3	-31.803 25	134.156 03	0.816	-317.750 1	254.143 6
		G4	536.499 25	134.156 03	0.001	250.552 4	822.446 1
		G5	-553.308 50	134.156 03	0.001	-839.255 3	-267.361 7
	G3	G1	1 006.559 00	134.156 03	0	720.612 2	1 292.505 8
		G2	31.803 25	134.156 03	0.816	-254.143 6	317.750 1
		G4	568.302 50	134.156 03	0.001	282.355 7	854.249 3
		G5	-521.505 25	134.156 03	0.001	-807.452 1	-235.558 4
	G4	G1	438.256 50	134.156 03	0.005	152.309 7	724.203 3
		G2	-536.499 25	134.156 03	0.001	-822.446 1	-250.552 4
		G3	-568.302 50	134.156 03	0.001	-854.249 3	-282.355 7
		G5	-1 089.807 75	134.156 03	0	-1 375.754 6	-803.860 9
	G5	G1	1 528.064 25	134.156 03	0	1 242.117 4	1 814.011 1
		G2	553.308 50	134.156 03	0.001	267.361 7	839.255 3
		G3	521.505 25	134.156 03	0.001	235.558 4	807.452 1
		G4	1 089.807 75	134.156 03	0	803.860 9	1 375.754 6

表 3 纤维桩组组内显著性的 LSD 分析检验

因变量	控制组	对比组	平均差	标准误	P 值	95% CI	
						下限值	上限值
纤维桩组	G1	G2	-1 152.263 50	199.731 87	0	-1 577.981 9	-726.545 1
		G3	-1 174.172 75	199.731 87	0	-1 599.891 2	-748.454 3
		G4	-618.451 75	199.731 87	0.007	-1 044.170 2	-192.733 3
		G5	-1 253.862 50	199.731 87	0	-1 679.580 9	-828.144 1
	G2	G1	1 152.263 50	199.731 87	0	726.545 1	1 577.981 9
		G3	-21.909 25	199.731 87	0.914	-447.627 7	403.809 2
		G4	533.811 75	199.731 87	0.017	108.093 3	959.530 2
		G5	-101.599 00	199.731 87	0.618	-527.317 4	324.119 4
	G3	G1	1 174.172 75	199.731 87	0	748.454 3	1 599.891 2
		G2	21.909 25	199.731 87	0.914	-403.809 2	447.627 7
		G4	555.721 00	199.731 87	0.014	130.002 6	981.439 4
		G5	-79.689 75	199.731 87	0.696	-505.408 2	346.028 7
	G4	G1	618.451 75	199.731 87	0.007	192.733 3	1 044.170 2
		G2	-533.811 75	199.731 87	0.017	-959.530 2	-108.093 3
		G3	-555.721 00	199.731 87	0.014	-981.439 4	-130.002 6
		G5	-635.410 75	199.731 87	0.006	-1 061.129 2	-209.692 3
	G5	G1	1 253.862 50	199.731 87	0	828.144 1	1 679.580 9
		G2	101.599 00	199.731 87	0.618	-324.119 4	527.317 4
		G3	79.689 75	199.731 87	0.696	-346.028 7	505.408 2
		G4	635.410 75	199.731 87	0.006	209.692 3	1 061.129 2

复体脱粘接,有且仅有 1 个 I 型断裂模式的牙齿存在于 G3,牙齿实际断裂图和光学显微镜图见图 5。

3 讨论

保存牙体组织是微创修复的一个关键方面,在

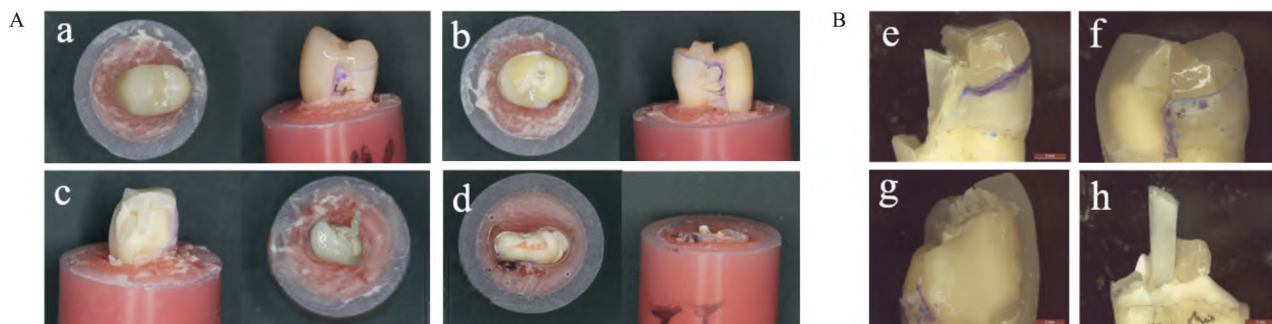


图5 断裂模式光学图及显微镜图

A: 断裂模式光学图(a: I型断裂; b: II型断裂; c: III型断裂; d: IV型断裂); B: 断裂显微镜图(e: 瓷贴面IV型断裂; f: 颊瓷贴面II型断裂; g: 颊邻瓷贴面III型断裂; h: 全冠IV型断裂)

修复无髓牙时,为保存牙齿结构而进行最小限度干预越来越受欢迎^[7]。穿髓型楔状缺损牙齿的寿命很大程度上取决于剩余健康牙齿组织的量。临床上,上颌前磨牙区的正常咬合力为222~445 N,咬合过程中的咬合力约为800 N^[8]。在本研究中,体外实验的最终结果表明,3种瓷贴面及全冠修复都能承受上颌前磨牙的正常咬合力,并远远超过最大咬合力,这与张樱等^[9]研究结果相同,进一步证明了穿髓型楔状缺损微创修复的可能性。

除正常咬合力外,冷热刺激和咬合疲劳也会影响无髓牙修复后的使用时间。Ozcan et al^[10]选择了1 200 000个循环周期来模拟5年的牙齿受力时间,为了减少操作时间,本研究选择了20 000个周期。同时,将半球形钛钢压头同时接触颊舌面,简化了牙齿复杂的尖窝接触又尽可能模拟实际受力^[11]。断裂数据显示,全冠组的断裂载荷最大,这与Huang et al^[12]的研究结果相反。这可能是由于本研究全冠的厚度比瓷贴面厚0.5 mm,而Huang et al将全冠厚度设为与瓷贴面厚度相同。瓷贴面和颊瓷贴面组的断裂载荷仅次于全冠组,颊邻瓷组的断裂载荷最小,这也证明了微创修复的可行性。研究^[13]表明,在严重磨损的牙齿上使用瓷贴面代替全冠,在人工老化后,这种微创修复设计确实显示出足够的强度来承受模拟的咀嚼功能。与牙釉质粘接的微创咬合嵌体陶瓷修复体的抗折性能远远高于与牙本质粘接的陶瓷修复体,甚至显示出与厚咬合贴面粘接在牙本质上的抗折性能相当。在本研究中,瓷贴面和颊瓷贴面仅与牙釉质表面粘接,而颊邻瓷贴面的近、远中面与牙本质粘接,同时,牙体组织磨除量相对较多,这就表明颊邻瓷组断裂载荷最小的原因。

对于断裂模式,大部分是牙齿和修复体的共同断裂,小部分是修复体的粘接断裂。其中,全冠组绝

大部分不可再次修复,具体断裂类型包括CEJ以下的牙冠横折、颊侧牙冠半折和颊向斜折等,其中牙冠横折的比例最高。瓷贴面组不可修复的比例仅次于全冠组,且实际断裂多为颊侧牙冠半折,颊瓷贴面及颊邻瓷贴面组断裂形式多为修复体脱粘接,且缺损处的树脂保存率最佳,这与Jurema et al^[14]的研究结果相符,充分表明了颊瓷贴面修复的优点,即牙齿预备量小、覆盖缺损处,断裂模式有利,同时也表明瓷贴面修复未能覆盖缺损处树脂的不足。

纤维桩组和树脂组组间两两比较的显著性结果显示,仅G4组组间断裂载荷比较差异有统计学意义($P < 0.05$),而其余四组均无显著性差异,与Magne et al^[15]的结果一致。G4组纤维桩增强整个牙齿系统的抗力作用明显,但预备过程中会进一步去除牙体组织,增加根管微裂纹。纤维桩组的不可修复断裂少于树脂组,断裂模式略优于树脂组,但考虑到微创修复,纤维桩是否应作为常规应用有待进一步研究。

综上所述,3种瓷贴面的最大断裂载荷均能承受上颌前磨牙的正常咬合力,颊瓷贴面的断裂载荷较高,且断裂模式有利,牙齿预备量小,是一种较好的修复穿髓型楔状缺损的方式;纤维桩不能显著增强穿髓型楔状缺损牙齿的断裂载荷。然而,本实验只研究了一种类型的穿髓型楔状缺损模型,且仅设置了“垂直”和“压缩”两个条件,而实际口腔中牙齿受力情况较复杂,收集的牙齿形态和大小上也不可避免的存在一些差异,本实验结果在临床上的实际应用还有待进一步研究。

参考文献

- [1] De Kok P, Pereira G K R, Fraga S, et al. The effect of internal roughness and bonding on the fracture resistance and structural reliability of lithium disilicate ceramic [J]. Dent Mater, 2018, 33

- (12): 1416–25.
- [2] Cieplik F, Scholz K J, Tabenski I, et al. Flowable composites for restoration of non-carious cervical lesions: results after five years [J]. *Dent Mater* 2019, 33(12): 428–37.
- [3] Heintze S D, Ruffieux C, Rousson V. Clinical performance of cervical restorations—a meta-analysis [J]. *Dent Mater* 2018, 26(10): 993–1000.
- [4] Almasri M. Assessment of extracting molars and premolars after root canal treatment: a retrospective study [J]. *Saudi Dent J* 2019, 31(4): 487–91.
- [5] Yazigi C, Schneider H, Chaar M S, et al. Effects of artificial aging and progression of cracks on thin occlusal veneers using SD-OCT [J]. *J Mech Behav Biomed Mater* 2018, 88: 231–7.
- [6] Guess P C, Schultheis S, Wolkewitz M, et al. Influence of preparation design and ceramic thicknesses on fracture resistance and failure modes of premolar partial coverage restorations [J]. *J Prosthet Dent* 2020, 110(4): 264–73.
- [7] Ioannidis A, Muhlemann S, Ozcan M, et al. Ultra-thin occlusal veneers bonded to enamel and made of ceramic or hybrid materials exhibit load-bearing capacities not different from conventional restorations [J]. *J Mech Behav Biomed Mater* 2021, 90: 433–40.
- [8] Ozcan M, Jonasch M. Effect of cyclic fatigue tests on aging and their translational implications for survival of all-ceramic tooth-borne single crowns and fixed dental prostheses [J]. *J Prosthodont*, 2018, 27(4): 364–75.
- [9] 张 樱, 张 宁, 赵卫芳, 等. IPS e-max Press 功能性牙合贴面抗折性和断裂模式的研究 [J]. *安徽医科大学学报*, 2021, 56(8): 1332–4.
- [10] Ozcan M, Jonasch M. Effect of cyclic fatigue tests on aging and their translational implications for survival of all-ceramic tooth-borne single crowns and fixed dental prostheses [J]. *J Prosthodont* 2018, 27(4): 364–75.
- [11] Schlichting L H, Resende T H, Reis K R, et al. Ultrathin CAD-CAM glass-ceramic and composite resin occlusal veneers for the treatment of severe dental erosion: An up to 3-year randomized clinical trial [J]. *J Prosthet Dent* 2022, 128(2): 158.
- [12] Huang X, Zou L, Yao R, et al. Effect of preparation design on the fracture behavior of ceramic occlusal veneers in maxillary premolars [J]. *J Dent* 2020, 97: 1033–46.
- [13] Skouridou N, Pollington S, Rosentritt M, et al. Fracture strength of minimally prepared all-ceramic CEREC crowns after simulating 5 years of service [J]. *Dent Mater* 2013, 29(6): e70–7.
- [14] Jurema A L B, Filgueiras A T, Santos K A, et al. Effect of intraradicular fiber post on the fracture resistance of endodontically treated and restored anterior teeth: a systematic review and meta-analysis [J]. *J Prosthet Dent* 2022, 128(1): 13–24.
- [15] Magne P, Goldberg J, Edelhoff D, et al. Composite resin core build-ups with and without post for the restoration of endodontically treated molars without ferrule [J]. *Oper Dent* 2016, 41(1): 64–75.

Study on the fracture resistance of preparation designs of occlusal veneer and fiber posts in pulp-penetrating wedge-shaped defects

Zhang Yuqing^{1,2}, Chen Ruting^{1,2}, Wu Guomin^{1,2}, Zhang Hongyan^{1,2}

(¹ Stomatological College of Anhui Medical University, The Affiliated Stomatological Hospital of Anhui Medical University, Anhui Province Key Laboratory of Oral Diseases Research, Hefei 230032; ² Dept of Dentistry and Pulp, The Affiliated Stomatological Hospital of Anhui Medical University, Hefei 230032)

Abstract Objective To investigate the effects of different occlusal veneer preparation designs and fiber posts on the fracture load and failure mode of endodontically treated maxillary premolars with pulp-piercing wedge-shaped defect. **Methods** 60 maxillary first premolars were randomly divided into group A and group B after Root Canal Therapy (RCT) and severe defects ($n = 30$). Group A was filled with glass fiber post and resin core, and group B was filled with resin core only. Then the occlusal veneer (G2), buccal-occlusal veneer (G3) and buccal-proximal-occlusal veneer (G4) were applied to the isolated teeth. The teeth filled with composite resin (G1) and full crown (G5) were set as negative and positive control respectively, with 6 samples in each group. The sample was subjected to 5 000 hot and cold cycles and 20 000 vertical compression load aging. Finally, all the samples were loaded with static load until the sample broke at the speed of 0.5 mm/min. The fracture load and failure mode of each sample were recorded. **Results** Both the fracture load in group A and B was $G5 > G3 > G2 > G4 > G1$, and the fracture load in G2, G3, G4, G5 was significantly higher than that in G1 ($P < 0.05$), and there was no significant difference between group A and B ($P > 0.05$). The fracture form of G3 was mostly unbonding of the repair body, which was conducive to re-repair. **Conclusion** Buccal (occlusal) veneer is the most effective in repairing pulp-piercing wedge-shaped defects. The fiber post could not significantly enhance the fracture load of the pulp-piercing wedge-shaped defects teeth.

Key words occlusal veneer; wedge-shaped defect; fracture load; failure mode